Magnetic correlations in a periodic Anderson model with nonuniform conduction electron coordination

N. Hartman, W.-T. Chiu, and R. T. Scalettar

Phys. Rev. B **93**, 235143 — Published 21 June 2016

DOI: 10.1103/PhysRevB.93.235143

Magnetic Correlations in a Periodic Anderson Model with Non-Uniform Conduction Electron Coordination

N. Hartman[1], W.-T. Chiu[2] and R.T. Scalettar[2]
[1]*Department of Physics, Southern Methodist University, Dallas, Texas 75275-0175 and*
[2]*Department of Physics, One Shields Ave., University of California, Davis, California 95616, USA*

The Periodic Anderson Model (PAM) is widely studied to understand strong correlation physics and especially the competition of antiferromagnetism and singlet formation. In this paper we extend QMC work on lattices with uniform numbers of neighbors to geometries in which the conduction electron sites can have variable coordination z. This situation is relevant both to recently discovered magnetic quasicrystals and also to magnetism in doped heavy fermion systems. Our key results are the presence of antiferromagnetic order at weak interorbital hybridization $V_{\rm fd}$, and a delay in singlet formation to larger values of $V_{\rm fd}$ on sites with larger z. The staggered magnetization tends to be larger on sites with higher z, providing insight into the behavior to be expected in crown, dice, and CaVO lattices.

PACS numbers: 71.10.Fd, 71.30.+h, 02.70.Uu

I. INTRODUCTION

The single band Hubbard Hamiltonian[1–4] captures several of the most fundamental consequences of electron-electron interactions in solids, namely magnetic order and the Mott metal-insulator transition. Multi-band Hamiltonians like the periodic Anderson model (PAM)[5,6] examine what happens when two species of electrons, one delocalized 'conduction' band (often d), and another localized band (often f) are present. Here a central effect is the competition between singlet formation[7], when the conduction and localized electrons are strongly hybridized, and ordering of the local moments mediated indirectly through the Ruderman-Kittel-Kasuya-Yosida interaction[8–11]. In heavy fermion materials[12,13], this competition is believed to explain different low temperature phases, e.g. non-magnetic $CeAl_3$ where the f moments are screened by the conduction electrons, and $CeAl_2$ which becomes antiferromagnetic (AF) at low temperatures.

Quantum Monte Carlo (QMC) studies of the PAM have explored some of this physics, in one[14,15], two[16], and three dimensions[17]. The focus has been on bipartite lattices which, at half-filling, host AF order without frustration and are also free of the fermion sign problem[18,19]. QMC in infinite dimensions[20] complements work in finite d by allowing simulations at very low temperature, at or even well below the Kondo scale, at the expense of some of the knowledge of correlations in space.

There is interest in understanding the magnetic correlations in more general geometries. One such modification allows for intersite, rather than on-site, hybridization between conduction and local orbitals and hence metallic behavior in the absence of interactions[21]. Another motivation is provided by chemical substitution in heavy fermion materials, either by the replacement of some of the local moment atoms by non-magnetic ones, as in $(Ce,La)CoIn_5$[22] or by changes to the conduction orbitals, as in the alloying of Cd onto In sites in $CeCo(In,Cd)_5$[23,24]. In the latter situation, $V_{\rm fd}$ is reduced locally, and AF droplets can form around the impurity sites.

A second motivation is the recent observation of a quantum critical state in magnetic quasicrystals[25,26]. In these Au-Al-Yb alloys ($Au_{51}Al_{34}Yb_{15}$), measurements of the magnetic susceptibility χ and specific heat C diverge as $T \to 0$. This non-Fermi liquid (NFL) behavior is associated with strongly correlated $4f$ Yb electrons. These two sets of materials share a common feature which is that the coordination number of the different atoms is no longer spatially uniform. The effects of these unique local environments can be probed with nuclear magnetic resonance[27].

The NFL behavior of Au-Al-Yb alloys has recently been studied by solving the $U = \infty$ Anderson Impurity Model (AIM) for a single local moment coupled to conduction electrons in a quasicrystal approximant geometry[28]. The crucial result is that singular responses in χ and C occur as a consequence of a broad (power law) distribution of Kondo temperatures which delays screening of a large fraction of the magnetic moments until very low temperatures.

In this paper we study the PAM in two different geometries: the Lieb lattice and a 2D "Ammann-Beenker" tiling[29,30]. Quasicrystaline approximates[32] for $Au_{51}Al_{34}Yb_{15}$ are in 3D; the quasi-periodic Ammann-Beenker tiling is a more tractable 2D alternative for QMC, which is limited in the number of sites which can be simulated.

Our goal here is to explore the nature of magnetic correlations as a function of f-d hybridization, and, specifically, to understand the competition of antiferromagnetic order and singlet formation in geometries where the coordination number of different sites in the lattice is non-uniform. Our work extends that of[28] by examining a dense array of local orbitals and also by including the effect of finite $U_{\rm f}$. We begin with the Lieb lattice, because it contains two separate

coordination numbers, $z = 2, 4$ while still retaining very simple lattice periodicity. We then turn to the more complicated quasicrystal approximant structure. We do not at present address the anomalous NFL behavior of the magnetic susceptibility, since those phenomena appear to be associated only with the quasicrystal itself, and not its approximant[24].

The magnetic properties of quantum antiferromagnets in geometries which have variable coordination number (quasicrysal, crown, and dice lattices) have also been studied in the context of the spin-1/2 Heisenberg Hamiltonian[31,33–35]. The general trend is to a reduction in order (eg. the staggered magnetization) on sites with larger z. On the other hand, in the case of *regular* geometries with uniform z, the ordered moment *increases* from the honeycomb and CaVO ($z = 3$) to square ($z = 4$) lattices[36]. We observe the latter trend here: spin-spin correlations grow with z. We will comment on this further in our conclusions.

Similar issues of magnetic order in quasicrystal lattices have also been explored in classical models. Ising spins coupled by Ruderman-Kittel-Kasuya-Yosida interactions[37] exhibit the somewhat surprising result of a low temperature phase with long range order, as opposed to glassy behavior. As in the quantum cases mentioned above, and studied in our work below, the magnetism is strongly dependent on the local environment. Meanwhile, the magnetic order of classical Heisenberg spins on a quasicrystal lattice is explored in[38].

II. MODEL AND METHODS

The PAM is a tight binding Hamiltonian for which each spatial site contains both an extended and a localized orbital,

$$\mathcal{H} = -t \sum_{\langle ij\rangle,\sigma} (d^\dagger_{i\sigma} d_{j\sigma} + d^\dagger_{j\sigma} d_{i\sigma}) - V_{\rm fd} \sum_{i\sigma} (d^\dagger_{i\sigma} f_{i\sigma} + f^\dagger_{i\sigma} d_{i\sigma}) + U_{\rm f} \sum_i (n^f_{i\uparrow} - \frac{1}{2})(n^f_{i\downarrow} - \frac{1}{2}) \quad (1)$$

Here t is the hybridization between conduction orbitals with creation(destruction) operators $d^\dagger_{i\sigma}(d_{i\sigma})$ on near neighbor sites $\langle ij\rangle$. In this paper we consider the two conduction electron geometries shown in Figs. 1,2 corresponding to "Lieb" and "quasicrystal" lattices respectively. Each site of these lattices also contains a localized orbital, creation(destruction) operators $f^\dagger_{i\sigma}(f_{i\sigma})$. $U_{\rm f}$ is the on-site interaction between spin up and spin down electrons on the localized orbital, and $V_{\rm fd}$ is the conduction-localized orbital hybridization. Both geometries of Figs. 1,2 are bipartite. In $\mathcal{H}$ we have written the interaction term, in 'particle-hole' symmetric form, and set the site energy difference between f and d orbitals to zero, so that the lattice is half-filled for all temperatures T and Hamiltonian parameters $t, U_{\rm f}, V_{\rm fd}$. Half-filling optimizes the tendency for AF correlations, and also allows DQMC simulations at low temperature since the sign problem[18] is absent.

Figure 3 shows the density of states and band structure of the PAM on a Lieb lattice for $t = 1$ and $V_{\rm fd} = 1$. There are six bands corresponding to the six sites (three conduction and three localized) per unit cell. The lattice is bipartite with four of the six sites on one sublattice and two on the other. Hence, in accordance with Lieb's theorem[39] there are two flat bands (at $E = \pm 1$). As in the case of the PAM on a square lattice with on-site hybridization, the half-filled lattice is a band insulator in the non-interacting limit. However, by comparing calculations for on-site and intersite $V_{\rm fd}$, the latter being metallic at half-filling, it has been shown that many properties of the PAM when $U_{\rm f}/t \gtrsim 4$ are insensitive to the presence of a $U_{\rm f}/t = 0$ band gap[21].

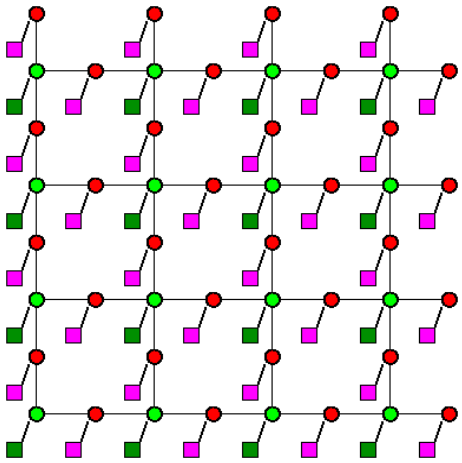

FIG. 1: (Color online) The Lieb lattice geometry under consideration in this paper. (Cluster shown has 4x4 unit cells with 48 sites). Each site contains both a conduction (d) orbital (circles) and a localized (f) orbital (squares), so that there is a total of 96 sites/orbitals. Horizontal and vertical lines correspond to the d-d hopping t. We use periodic boundary conditions (pbc). There are two possible conduction orbital coordinations, $z = 2, 4$. The local f orbitals are connected to the d orbital on the same site by hybridization $V_{\rm fd}$ (diagonal lines).

The magnetic properties of the PAM are characterized by intra- and inter-orbital spin-spin correlations,

$$c^{zz'}_{\rm ff}(r) = \langle f^\dagger_{i+r\downarrow} f_{i+r\uparrow} f^\dagger_{i\uparrow} f_{i\downarrow}\rangle$$
$$c^{zz'}_{\rm dd}(r) = \langle d^\dagger_{i+r\downarrow} d_{i+r\uparrow} d^\dagger_{i\uparrow} d_{i\downarrow}\rangle$$
$$c^{zz'}_{\rm fd}(r) = \langle f^\dagger_{i+r\downarrow} f_{i+r\uparrow} d^\dagger_{i\uparrow} d_{i\downarrow}\rangle \quad (2)$$

Here the superscripts z, z' refer to the coordination number of the conduction orbital on site i and $i + r$ respectively. This separation allows us to isolate the effects of the number of neighbors on the spin correlations[40]. We focus here on $c^{zz'}_{\rm ff}(r)$ which measures intersite magnetic correlations between the local electrons, and $c^{zz}_{\rm fd}(r = 0)$, the singlet correlator

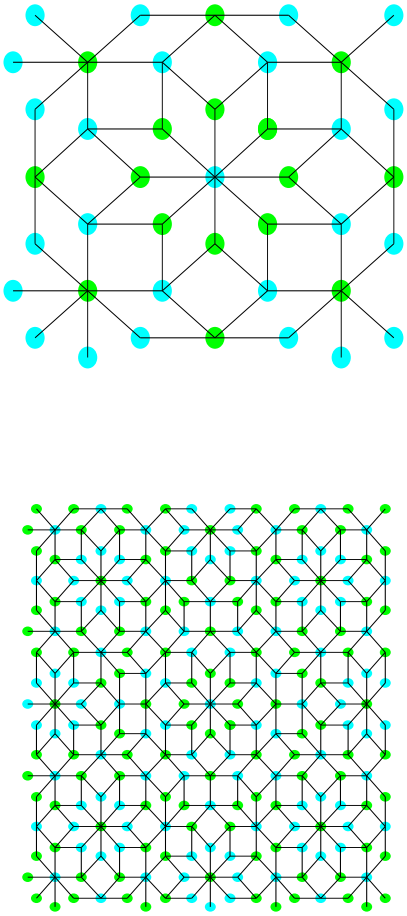

FIG. 2: (Color online) Top (bottom): Approximants to the $Au_{51}Al_{34}Yb_{15}$ crystalline lattice for $N = 41(239)$ sites. In each case, sites shown contain both a conduction (d) orbital and a localized (f) orbital. Because of the more complex (irregular) structure, we show only the conduction sites (circles) explicitly. There is a partner localized site, not shown, for each, the analogs of the squares in Fig. 1. Lines correspond to the d-d hopping t. The local f orbitals are connected to the d orbital on the same site by hybridization $V_{\rm fd}$. For this geometry we use open boundary conditions (OBC) to avoid frustration. The conduction electron sites range in coordination from $z = 1$ to $z = 8$. The use of two colors for the sites emphasizes that, despite its complexity, the geometry is still bipartite.

between local and conduction electrons on the same site. The spin-spin correlations are translationally invariant for uniform geometries and periodic boundary conditions, but depend more generally on both i and r in irregular lattices.

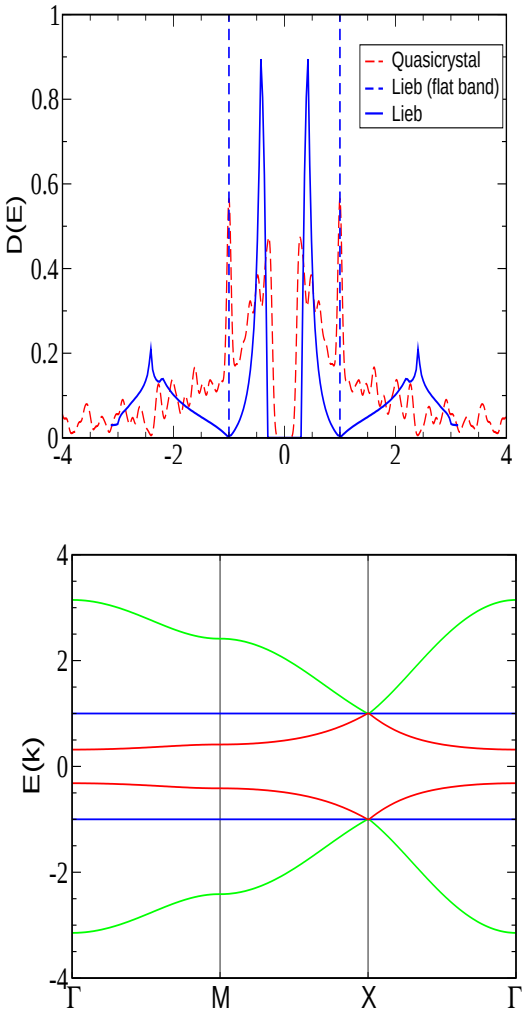

FIG. 3: (Color online) DOS (top) and band structure (bottom) of the PAM on a Lieb lattice. Here $t = 1$ and $V_{\rm fd} = 1$. The two completely flat bands at $E = \pm 1$ give rise to δ function spikes in $D(E)$ which are indicated by dashed vertical lines). $D(E = 0)$ vanishes: the system is a band insulator at half-filling. The DOS for the $N = 239$ quasicrystal approximant is also shown in the top panel. As is the case for the Lieb lattice PAM, the quasicrystal PAM also has a hybridization gap at $E = 0$. The single band case is metallic[28,35].

We also measure the structure factor,

$$\mathcal{S}^z_{\rm ff} = \sum_r \sum_{z'} c^{zz'}_{\rm ff}(r)(-1)^r$$
$$\mathcal{S}^{\rm tot}_{\rm ff} = \sum_r \sum_{zz'} g^{zz'} c^{zz'}_{\rm ff}(r)(-1)^r \qquad (3)$$

which sums the spin-spin correlations to all distances r from sites i with a given z. The staggered phase factor

$(-1)^r$ takes the value ± 1 on the two sublattices of the bipartite geometry and hence measures AF order. The z-resolved contributions to the total structure factor $S_{\rm ff}^{\rm tot}$ are weighted by the fractions of sites in the lattice with a given coordination $g^{zz'}$. In the singlet phase, the spin correlations decay exponentially with separation r and $S_{\rm ff}^{\rm tot}$ gets contributions only from a small number $r < \xi$ of local correlations. It becomes temperature independent below a relatively high T set by the singlet energy scale. In an ordered phase, on the other hand, $S_{\rm ff}^{\rm tot}$ will depend on temperature down to much lower T as the correlation length ξ diverges. Thus a T dependence of $S_{\rm ff}^{\rm tot}$ can be used as an initial indicator of AF order.

To determine the possibility of long range order in the ground state, we follow the seminal analysis of Hirsch and Tang[41] in their study of the two dimensional Hubbard model. The essence of the procedure is the observation that the correlation length $\xi(T)$ diverges as $T \to 0$, so that if one lowers T sufficiently one can satisfy the condition $\xi >> L$: the correlation length is much larger than the linear lattice size L. The required T will, of course, decrease as L increases. If one does this for a collection of L, one has a set of measurements which is in the ground state for each L. These results can then be extrapolated to $L = \infty$ to infer the ground state properties in the thermodynamic limit. As we shall discuss, a challenge which makes the PAM more difficult than the single band Hubbard model is the smallness of the RKKY interaction for weak interorbital hybridization $V_{\rm fd}$, which necessitates a very large β.

Our computational approach is determinant Quantum Monte Carlo (DQMC)[42,43]. This method allows the solution of interacting tight-binding Hamiltionians like the PAM through an exact mapping onto a problem of non-interacting particles moving in a space and (imaginary) time dependent auxiliary field. This field is sampled stochastically to obtain the expectation values of different correlation functions. The update moves require the non-local computation of the fermion Green's function, which also the quantity needed to measure equal time observables including the energy, double occupation, and spin correlations. The algorithm involves matrix operations and scales as the cube of the product of the number of spatial lattice sites and the number of orbitals. In certain special situations, including the PAM on the geometries studied here, the sampling is free of the sign problem[18] so that the simulation may be conducted on large lattices (here several hundreds of spatial sites) at low temperature (here $T/t \lesssim 1/30$).

III. PAM ON THE LIEB LATTICE

We begin with the Lieb lattice which has $2N/3$ sites of coordination number $z = 2$ and $N/3$ sites with $z = 4$. Figure 4 shows $c_{\rm ff}^{zz'}(r)$ for $V_{\rm fd} = 0.8$ and $V_{\rm fd} = 1.3$. In the former case, the correlation function alternates between positive and negative values, with a correlation length which exceeds the linear lattice size, as is characteristic of an AF phase. $r = 1$ corresponds to the separation between unit cells, so that integer values of r are between sites with $z' = z$ (and hence the same sublattice) and half-integer values have $z' \neq z$ (and hence occupy different sublattices). The AF correlations are evident in both $z = 2$ and $z = 4$, although they are larger for higher coordination number. This reflects the collective nature of the AF order, which is more robust as the number of neighbors grows. Actually, because the $\mathcal{A}$ and $\mathcal{B}$ sublattices have different numbers, the ordered phase is Ferrimagnetic[39], with $N_\uparrow \neq N_\downarrow$ in addition to the staggered pattern seen in the Figure. For $V_{\rm fd} = 1.3$, on the other hand, $c_{\rm ff}^{zz'}(r)$ falls rapidly to zero, indicative of a singlet phase.

The AF and singlet regimes can also be distinguished by $c_{\rm fd}^{zz}(r = 0)$, as shown in Fig. 5. (Here since $r = 0$ the coordination numbers $z' = z$.) $c_{\rm fd}^{zz}(r = 0)$ vanishes for $V_{\rm fd} = 0$ where the localized and conduction fermions are decoupled, and saturates at a large value for $V_{\rm fd} \to \infty$. For the sites with larger coordination number $z' = z = 4$, singlet correlations develop at larger V_{fd} than for sites with $z' = z = 2$. As might be expected for a local quantity, the singlet correlator for the $z = 4$ sites matches quite well to those on a square lattice. (The 4×4 square lattice is anomalous because of its unusual additional symmetries, and is not shown.)

In Fig. 6 we turn to the AF structure factor, Eq. 3, which sums the spin correlations on the localized orbitals over the whole lattice. In the singlet phase, $c_{\rm ff}^{zz'}(r)$ is short ranged and temperature independent, achieving its ground state value at $T \sim V_{\rm fd}^2/U_{\rm f}$. In the AF phase, on the other hand, the correlation length grows as T is lowered, and hence $c_{\rm ff}^{zz'}(r)$ contributes to the structure factor out to larger and larger distances. The structure factor becomes temperature dependent at low T. These two regimes are evident, and are separated by $V_{\rm c} \sim 1.1$. This is suggestive, but certainly not conclusive, evidence of the presence of a QCP. At the end of the following section we will provide a finite size scaling analysis of this data to ascertain whether there is true long range order below $V_{\rm c}$. Note that the reduction in $S_{\rm ff}^{\rm tot}$ as V_{fd} is reduced below $V_{fd} \approx 0.7$ is a finite temperature effect. The RKKY exchange scales as V_{fd}^2 and $T = t/30$ ($\beta t = 30$) is no longer low enough to reach the ground state.

IV. PAM ON A QUASICRYSTAL LATTICE

We turn now to the quasicrystal geometry. Our discussion will parallel that of the preceding section. For this lattice, the choices for coordination number are more numerous, $z = 1, 2, \cdots 8$, as evident in Fig. 2. The $z = 1, 2$ sites originate in our use of OBC, a choice made to avoid frustration of AF order[44]. It is important to emphasize that these coordination numbers occur only at the lattice edges. Their contribution to the properties

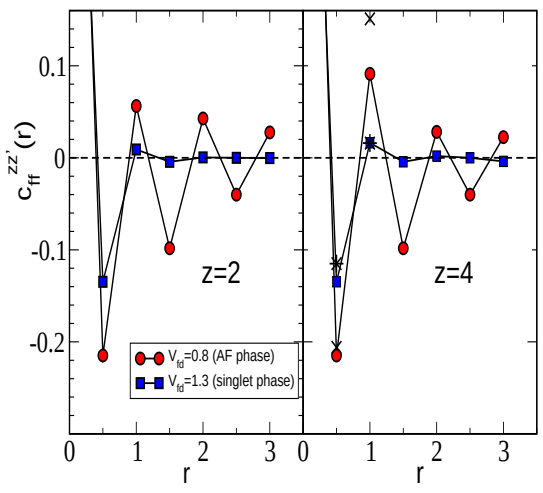

FIG. 4: (Color online) Spin-spin correlation function $c_{\rm ff}^{zz'}(r)$ as a function of r for the half-filled Lieb lattice with $U_{\rm f} = 4t$ and $\beta = 30$. $r = 1$ is the unit cell size: integer r correspond to $z' = z$ and half-integer values to $z' \neq z$. The red(blue) symbols show $V_{\rm fd} = 0.8t(1.3t)$ respectively. For $V_{\rm fd} = 0.8t$ there is AF order to large r, while for $V_{\rm fd} = 1.3$, $c_{\rm ff}^{zz'}(r)$ decays rapidly to zero. In the AF regime, larger z increases $c_{\rm ff}^{zz'}(r)$. Data depicted by x ($V_{\rm fd} = 0.8$) and $*$ ($V_{\rm fd} = 1.3$) are for the square lattice. $r = 0.5$ is for near-neighbors, and $r = 1.0$ for next near-neighbors.

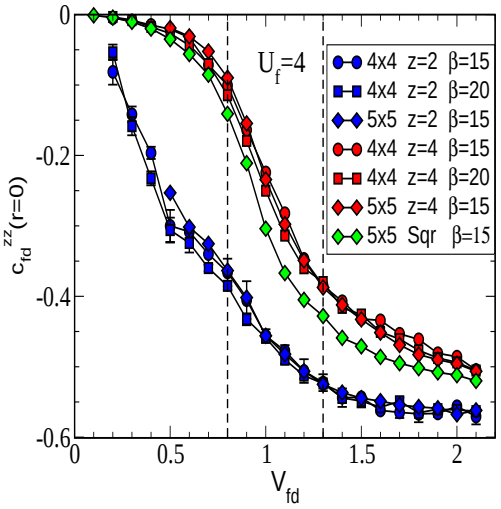

FIG. 5: (Color online) Local singlet correlator $c_{\rm fd}^{zz'}(r = 0)$ for the half-filled Lieb lattice with $U_{\rm f} = 4t$. The singlet correlations develop more rapidly for $z = 2$ than for $z = 4$ since for smaller coordination number the competition with AF order is reduced. Data for different ($\beta = 15, 20$) as well as different system sizes (4x4 and 6x6) overlap: this short range correlation function converges rather quickly as T is lowered and N is increased. Vertical dashed lines at $V_{fd} = 0.8, 1.3$ demark the values used for the real space spin correlation data of Fig. 4. Square lattice data coincide well with Lieb sites with $z = 4$.

of the system will vanish in the thermodynamic limit.

$c_{\rm ff}^{zz'}(r)$ for the quasi-crystal geometry is given in Fig. 7 and shows a differentiation between long range behavior for $V_{\rm fd} = 0.8$ and rapid decay to zero for $V_{\rm fd} = 1.4$. Similar to the Lieb case, $c_{\rm ff}^{zz'}(r)$ is larger for $z = 4$ than $z = 2$. Data for other z (not shown) confirm this trend. The AF correlations extending outward from a site become more and more robust as the coordination number of the conduction orbital increases.

Figure 8 shows the singlet correlator for the $N = 239$ site quasicrystal geometry of Fig. 2(bottom). The appearance of well-formed singlets depends on the coordination number z of the conduction electron site-the point of maximum change of $c_{\rm fd}^{z}(r = 0)$ shifts from $V_{\rm fd} \sim 0.4$ to $V_{\rm fd} \sim 1.1$ as z increases. This reflects the fact that AF is favored by a larger number of neighbors, so that the cross-over to singlets requires larger $V_{\rm fd}$ as z increases. Since $c_{\rm fd}^{zz}(r = 0)$ is a local quantity, its value is relatively unaffected by total lattice size (data in Fig. 8 for $N = 41$ and $N = 239$ are similar), and it also converges with β fairly quickly. (Data in Fig. 8 for $\beta = 15$ and $\beta = 20$ are similar).

The sum of the spin-spin correlation function of localized fermions in the quasi-crystal geometry yields the structure factor and is given in Fig. 9 as a function of $V_{\rm fd}$. For hybridizations $V_{\rm fd} \gtrsim 1.1$, where results in Fig. 8 suggest singlet formation is robust for all z, $S_{\rm ff}^{\rm tot}$ is temperature independent. Below $V_{\rm fd} \sim 1.1$, curves for different β break apart, suggesting that AF correlations are present and increasing as T is lowered. As noted in the discussion of Fig. 6, the reduction in the structure factor at low $V_{\rm fd}$ is a finite temperature effect: the effective RKKY coupling goes as $V_{\rm fd}^2$ and hence even larger β is needed for AF correlations to develop at small $V_{\rm fd}$. See also[45].

In the presence of long range order (LRO) the correlation approaches a nonzero asymptotic value $c(r \to \infty) \to m^2$, where m is the order parameter, and the structure factor scales as $S = Nm^2$. Even if LRO is present only at $T = 0$, as is the cases in $d = 2$ with continuous symmetries, this scaling is observed at T low enough that the correlation length exceeds the largest linear lattice size studied. We expect $S > Nm^2$ on finite lattices, since $c(r) > m^2$ at small distances, and these short range contributions can be substantial if the lattice size is small. A finite size scaling plot for the Lieb lattice is given in Fig. 10.

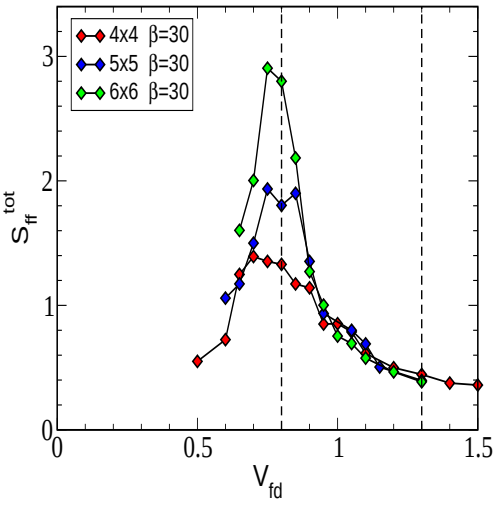

FIG. 6: (Color online) Localized electron antiferromagnetic structure factor for the Lieb lattice. For $V_{\rm fd} \gtrsim 1.1$, $S_{\rm ff}^{\rm tot}$ is independent of temperature and lattice size N. However, when T is decreased for $V_{\rm fd} \lesssim 1.1$, $S_{\rm ff}^{\rm tot}$ grows as the system is cooled. These distinct behaviors reflect the completely local nature of magnetic correlations in the singlet phase, and an increasing correlation length at low T in the AF phase. Vertical dashed lines at $V_{fd} = 0.8, 1.3$ demark the values used for the real space spin correlation data of Fig. 4.

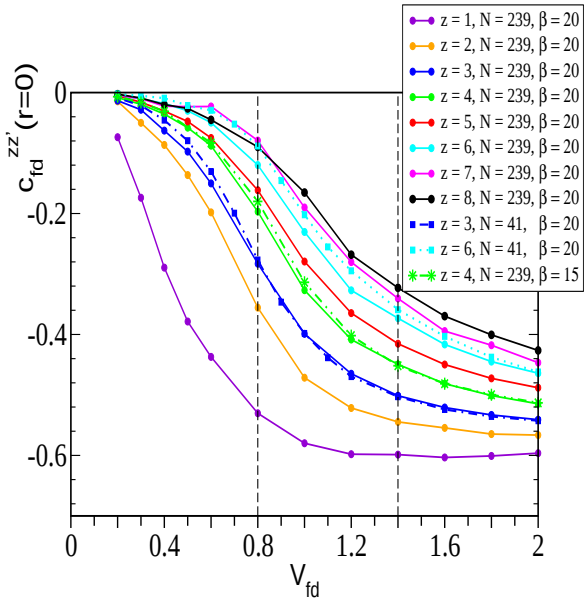

FIG. 8: (Color online) The singlet correlators (circles) for the quasicrystal geometry with $N = 239$ sites and inverse temperature $\beta = 20$ shown as functions of $V_{\rm fd}$. $c_{fd}^{z}(r = 0)$ is largest in magnitude for smallest $z = 1$. The singlets become less and less well-formed as z increases. Data for $N = 41$ sites (squares) indicate that finite size effects are relatively small. Similarly, data for $\beta = 15$ (diamonds) show that the low T limit has been reached. Vertical dashed lines show the $V_{\rm fd}$ values of Fig. 7.

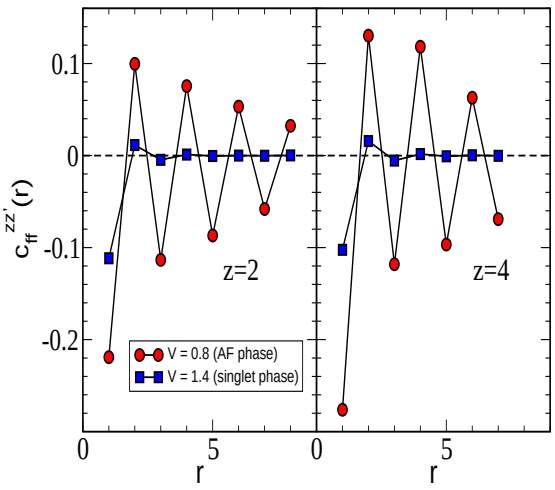

FIG. 7: (Color online) z resolved spin-spin correlation function between localized orbitals for $V_{\rm fd} = 0.8$ (AF phase) and $V_{\rm fd} = 1.4$ (singlet phase) for the $N = 41$ quasicrystal lattice at $\beta = 30$. In the former case, $c_{\rm ff}^{z}(r)$ remains non-zero out to large separations, while in the latter case it falls off to zero. Left(right) panels are $z = 2(4)$.

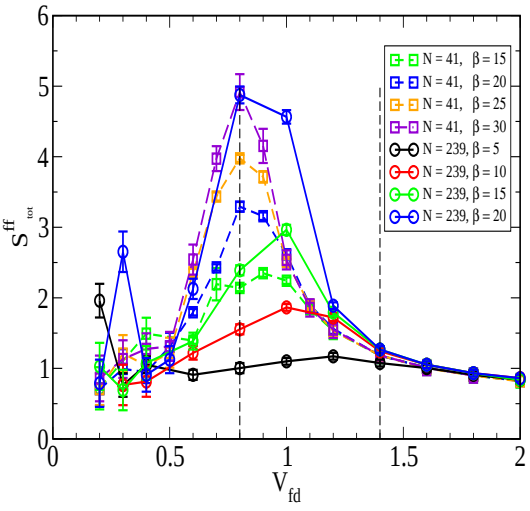

FIG. 9: (Color online) $S_{\rm ff}^{\rm tot}$ as a function of $V_{\rm fd}$ for several inverse temperatures β and quasicrystal lattice sizes $N = 41, 239$. As for the Lieb lattice, curves coincide for different β in the singlet phase at large $V_{\rm fd}$, but break apart at $V_{\rm fd} \approx 1.0 - 1.1$. This signals the development of antiferromagnetic correlations at large spatial separations at low $V_{\rm fd}$. Vertical dashed lines show the $V_{\rm fd}$ values of Fig. 7.

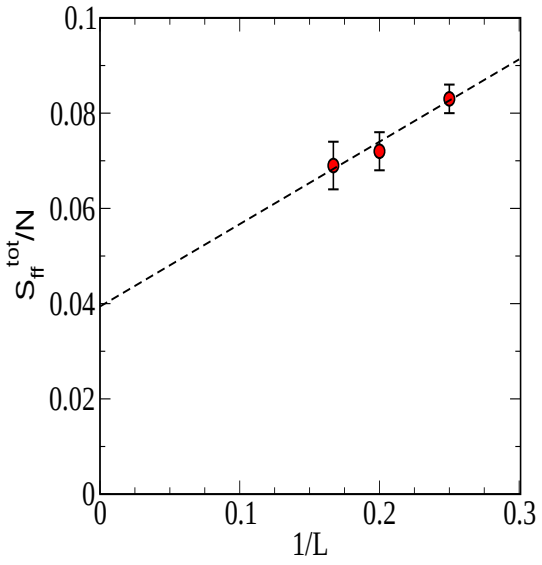

FIG. 10: (Color online) Finite size scaling plot for the PAM on the Lieb lattice. Using 4x4, 6x6, and 8x8 unit cells, the normalized structure factor $S_{\rm ff}^{\rm tot}/N$ scales to a nonzero value for $V_{\rm fd} = 0.8$. Here the inverse temperature $\beta = 30$ which is large enough that ground state properties have been reached for lattices of the sizes shown.

V. CONCLUSIONS

We have explored the competition between antiferromagnetic order and singlet formation in the periodic Anderson model in 2D geometries which are unfrustrated, but which have conduction electron coordination which varies from site to site. As is intuitively reasonable, singlet formation depends on z, and is delayed to larger interorbital hybridization $V_{\rm fd}$ as z increases. Our data suggest that, as in the case of uniform z, AF order is present in the ground state at low $V_{\rm fd}$ and absent at large $V_{\rm fd}$. Related issues arise in models in which site dilution provides different conduction electron coordination[46,47] or in which variation in conduction electron-local orbital hybridization is considered[48].

As noted in the introduction, the staggered moment tends to go *down* with increasing z in the spin-1/2 Heisenberg model on quasicrystal lattices[30,33–35]. Our work differs from those studies in two respects. First, we consider itinerant, rather than localized spins. Second, we consider a model with two moments per site, one associated with the conduction electron band and one with the local band. It is not completely clear which of these differences is responsible for the alteration in the effect of local z on the spin correlations. It might be of interest to study a single band (Hubbard) model with variable z to isolate the answer to this question.A number of experimental systems also exhibit a similar behavior in which T_{Neel} can be higher at the (lower z) surface than in the (higher z) bulk.[49] Our work, and much of the literature, has considered models with variable z which, however, remain bipartite. The combined of frustration and variable z are studied in[36].

Both geometries studied have unusual $U_{\rm f} = 0$ single particle eigenstates. In the case of the Lieb lattice, the inequivalence of the number of sites in the A and B sublattices leads to the presence of flat bands. In the true quasicrystal geometry (of which we explore only an approximant) the eigenstates exhibit an intermediate scaling with system size, between the limits where the participation ratio $\mathcal{P}$ grows with the number of sites, as occurs for Bloch states, and $\mathcal{P} \sim o(1)$ for conventional localization[24,28]. Thus our work also explores the effects of those features of the noninteracting spectrum on magnetic correlations in the presence of interactions.

Limitations on accessible system sizes and temperatures prevent us from addressing high precision questions such as whether the distribution of z destroys a sharp quantum critical point (QCP) between the AF and singlet phases and replaces it with a more gradual cross-over. Related DMFT work[28] indicates that there is a range of Kondo temperatures. It is interesting to note that, to within the accuracy DQMC simulations provide, there is remarkably little variation between the critical value of $V_{\rm fd}$ for different 2D conduction electron geometry. The QCP appears to be quite close to the square lattice value $V_{\rm fd}/t \approx 1$ for the Lieb and quasicrystal lattices considered here.

The usual view of the PAM is of a two band (conduction and localized) tight binding Hamiltonian. Although we have emphasized here the presence of sites with different conduction electron lattice coordination numbers, an alternate perspective on our work is that of a study of a PAM in which the conduction electrons themselves have several bands. The Lieb lattice geometry, for example, has three sites per unit cell, and hence three conduction bands (Fig. 3), in addition to the localized orbitals. Our DQMC simulations indicate that the competition between singlet formation and AF order is not fundamentally affected by this more complex band structure.

VI. ACKNOWLEDGEMENTS

The work of NH was supported by NSF-PHY-1263201 (REU program). RTS and WTC were supported by DE-SC0014671. We are grateful to Eric Andrade and Vladimir Dobrosavljevic for useful conversations.

[1] *The Hubbard Model- Recent Results*, M. Rasetti, World Scientific, 1991.

[2] "*The Hubbard Model*," Arianna Montorsi (ed), World Scientific, 1992.

[3] *The Mott Metal-Insulator Transition, Models and Methods*, F. Gebhard, Springer 1997.

[4] *Lecture Notes on Electron Correlation and Magnetism*, P. Fazekas, World Scientific (1999).

[5] P.W. Anderson, Phys. Rev. 124, 41 (1961).

[6] S. Doniach, Physica 91B, 231 (1977); B. Cornut and B. Coqblin, Phys. Rev. B5, 441 (1972).

[7] J. Kondo, Solid State Phys. 23, 183 (1969).

[8] M.A. Ruderman and C. Kittel, Phys. Rev. 96, 99 (1954).

[9] T. Kasuya, Prog. Theor. Phys. 16, 45 (1956).

[10] K. Yosida, Phys. Rev. 106, 893 (1957).

[11] C. Kittel, *Quantum Theory of Solids*, (Wiley, New York, 1963).

[12] G.R. Stewart, Rev. Mod. Phys. 56, 755 (1984).

[13] G.R. Stewart, Rev. Mod. Phys. 73, 797 (2001).

[14] R. Blankenbecler, J.R. Fulco, W. Gill, and D.J. Scalapino, Phys. Rev. Lett. 58, 411 (1987).

[15] R.M. Fye, Phys. Rev. B41, 2490 (1990)

[16] M. Vekic, J.W. Cannon, D.J. Scalapino, R.T. Scalettar, and R.L. Sugar, Phys. Rev. Lett. 74, 2367 (1995).

[17] C. Huscroft, A.K. McMahan, and R.T. Scalettar, Phys. Rev. Lett. 82, 2342 (1999).

[18] E.Y. Loh, J.E. Gubernatis, R.T. Scalettar, S.R. White, D.J. Scalapino, and R.L. Sugar, Phys. Rev. B41, 9301 (1990).

[19] Matthias Troyer and Uwe-Jens Wiese, Phys. Rev. Lett. 94, 170201 (2005).

[20] M. Jarrell, H. Akhlaghpour, and T. Pruschke, Phys. Rev. Lett. 70, 1670 (1993).

[21] K. Held, C. Huscroft, R.T. Scalettar, and A.K. McMahan, Phys. Rev. Lett. 85, 373 (2000).

[22] S. Nakatsuji, S. Yeo, L. Balicas, Z. Fisk, P. Schlottmann, P.G. Pagliuso, N.O. Moreno, J.L. Sarrao, and J.D. Thompson, Phys. Rev. Lett. 89, 106402 (2002).

[23] S. Seo, X. Lu, J-X. Zhu, R.R. Urbano, N. Curro, E.D. Bauer, V.A. Sidorov, L.D. Pham, T. Park, Z. Fisk, and J.D. Thompson, Nat. Phys. 10, 120 (2014).

[24] S. Seo, X. Lu, J-X. Zhu, R.R. Urbano, N. Curro, E.D. Bauer, V.A. Sidorov, L.D. Pham, T. Park, Z. Fisk, and J.D. Thompson, Nature Physics 110, 120 (2014).

[25] K. Deguchi, S. Matsukawa, N.K. Sato, T. Hattori, K. Ishida, H. Takakura, and T. Ishimasa, Nature Materials 11, 1013 (2012).

[26] T. Watanuki, S. Kashimoto, D. Kawana, T. Yamazaki, A. Machida, Y. Tanaka, and T. J. Sato, Phys. Rev. B 86, 094201 (2012).

[27] N.J. Curro, Rep. Prog. Phys. 72, 026502 (2009).

[28] E.C. Andrade, A. Jagannathan, E. Miranda, M. Vojta, and V. Dobrosavljevic, Phys. Rev. Lett. 115, 036403 (2015).

[29] U.W. Grimm and M. Schreiber, in *Quasicrystals - Structure and Physical Properties*, ed. H.-R. Trebin (Wiley-VCH, Weinheim, 2003), pp. 210-235.

[30] A. Jagannathan and F. Piéchon, Phil. Mag. 87, 2389 (2006).

[31] A. Jagannathan, Phys. Rev. Lett. 92, 047202 (2004).

[32] A quasicrystal approximant is a periodic crystal whose atomic arrangement shares the local structure of the quasicrystal. See "Quasicrystals and crystalline approximants", A.I. Goldman and R.F. Kelton, Rev. Mod. Phys. 65, 213 (1993).

[33] S. Wessel, A. Jagannathan, and S. Haas, Phys. Rev. Lett. 90, 177205 (2003).

[34] S. Wessel and I. Milat, Phys. Rev. B71, 104427 (2005).

[35] A. Jagannathan, R. Moessner, and Stefan Wessel, Phys. Rev. B 74, 184410 (2006).

[36] "Quantum s=12 antiferromagnets on Archimedean lattices: The route from semiclassical magnetic order to nonmagnetic quantum states" D.J.J. Farnell, O. G̈tze, J. Richter, R. F. Bishop, and P. H. Y. Li Phys. Rev. B89, 184407 (2014).

[37] Stefanie Thiem and J. T. Chalker, Phys. Rev. B92, 224409 (2015).

[38] E. Y. Vedmedenko, U. Grimm, and R. Wiesendanger Phys. Rev. Lett. 93, 076407 (2004).

[39] E.H. Lieb, Phys. Rev. Lett. 62, 1201 (1989).

[40] One could, of course, also separate the spin correlations based on the coordination number z' of the site $i+r$. In the case of the Lieb lattice, where there are only two pairs of choices $z, z' = 1, 2$ this would be feasible, but in the case of the quasicrystal geometry where $z, z' = 1, 2, \cdots 8$ such a refined breakdown would probably do more to obscure the analysis of the physics than to clarify it.

[41] J.E. Hirsch and S. Tang, Phys. Rev. Lett. **62**,591 (1989).

[42] R. Blankenbecler, D.J. Scalapino, and R.L. Sugar, Phys. Rev. D24, 2278 (1981).

[43] J.E. Hirsch, Phys. Rev. B31, 4403 (1985).

[44] PBC are usually employed to reduce finite size effects and give a more rapid approach to the thermodynamic limit, since they eliminate special features like reduced coordination number of sites at the lattice boundary. In the quasicrystal lattice, which has a distribution of z even in the absence of OBC, it is less clear that PBC are to be preferred. Furthermore, frustration which would be introduced by the use of PBC would cause the formation of domain walls which would have a similar large finite size effect as OBC.

[45] T. Paiva, G. Esirgen, R.T. Scalettar, C. Huscroft, and A.K. McMahan, Phys. Rev. B68, 195111 (2003).

[46] A.W. Sandvik, Phys. Rev. Lett. 96 207201 (2006).

[47] Kaj H. Höglund, A.W. Sandvik, and S. Sachdev, Phys. Rev. Lett. **98**, 087203 (2007)

[48] A.H. Castro-Neto, G. Castilla, and B.A. Jones, Phys. Rev. Lett. 81, 3531 (1998).

[49] F. Zhang, S. Thevuthasan, R.T. Scalettar, R.R.P. Singh, and C.S. Fadley, Phys. Rev. B51, 12468 (1995).